



Teaser Microfluidic technology offers an excellent alternative for current in vitro models. This review examines the impact of microfluidic systems on chemotherapeutic studies as a basis for diminishing the gap between in vivo and in vitro models.



Microfluidic technologies for anticancer drug studies

Karolina P. Valente^{1,4}, Sultan Khetani², Ahmad R. Kolahchi², Amir Sanati-Nezhad², Afzal Suleman¹ and Mohsen Akbari^{1,3,4}

¹ Department of Mechanical Engineering, University of Victoria, Victoria, BC, V8P 5C2, Canada

² Center for Bioengineering Research and Education, Department of Mechanical Engineering, University of Calgary, Calgary AB, T2N 1N4, Canada

³ Center for Biomedical Research, University of Victoria, Victoria, BC, V8P 5C2, Canada

⁴ Center for Advanced Materials and Related Technologies, University of Victoria, Victoria, BC, V8P 5C2, Canada

The study of cancer growth mechanisms and the determination of the efficacy of experimental therapeutics are usually performed in two-dimensional (2D) cell culture models. However, these models are incapable of mimicking complex interactions between cancer cells and the environment. With the advent of microfluidic technologies, the combination of multiple cell cultures with mechanical and biochemical stimuli has enabled a better recapitulation of the three-dimensional (3D) tumor environment using minute amounts of reagents. These models can also be used to study drug transport, hypoxia, and interstitial pressure within the tumor. In this review, we highlight the applications of microfluidic-based models in anticancer drug studies and provide a perspective on the future of the clinical applications of microfluidic systems for anticancer drug development.

Introduction

Cancer is a devastating disease that affects millions of people every year. According to the American Cancer Society, more than 1.6 million new cases of cancer were expected for 2016 and more than 0.5 million people were expected to die from cancer that year [1]. According to the National Cancer Institute, by 2024, almost 19 million people are expected to be living beyond a cancer diagnosis [2]. Owing to the evident increase of people diagnosed with cancer and undergoing treatment (14.5 million Americans in 2014), the National Expenditures for Cancer Care in the USA is projected to grow from US\$125 billion in 2010 to US\$156 billion in 2020. Even though cancer is often referred to as a single disease, it comprises hundreds of diseases that have a main factor in common: uncontrolled cell growth. This set of diseases arises from mutations in the DNA of a cell caused by genetic and environmental factors. Cancer defies the most basic behavior of normal cells, such as controlled division, specialized character situated in a specific location of the body, and survival for as long as required. Instead, cancer cells proliferate

Karolina Papera

Valente received her MSc in chemical engineering from Instituto Superior Tecnico, University of Lisbon, Portugal. Her MSc thesis focused on the study of mass transfer in extracorporeal membrane blood oxygenators and in the fabrication of polyurethane membranes. She is currently a PhD student in the Mechanical Engineering Department at University of Victoria, Canada. Her current research interests include microfluidic devices for biomedical applications.



Afzal Suleman

received his PhD from the mechanical engineering department at the University of British Columbia, Canada. He is currently Canada Research Chair and professor in computational and experimental mechanics at the University of Victoria, BC. He served as a NRC post-doctoral research fellow at the US Air Force from 1992–1994. He has also served as Associate Dean Research (2005–2009) and Associate Vice-President Research (2009–2010). His research interests include computational and experimental analysis of advanced engineering systems. He is a Fellow of the Canadian Academy of Sciences, of the Royal Aeronautical Society, and of the Royal Academy of Sciences Lisbon.



Mohsen Akbari

is an assistant professor of mechanical engineering and the director of Laboratory for Innovations in Microengineering (LiME) at the University of Victoria. He is also a member of the Center for Biomedical Research (CBR) and Center for Advanced Materials and Related Technology (CAMTEC) at the University of Victoria, Canada. Dr Akbari is internationally renowned for his innovations in microscale technologies, tissue engineering, and drug delivery. Dr Akbari's research interests include the development of advanced microfluidic systems for applications in tissue engineering, biosensing, wound healing, and cancer research.



Corresponding author: Akbari, M. (makbari@uvic.ca)

uncontrollably, invade territories of healthy cells, and affect the functionalization of different organs. Some cancer cells have the ability to migrate from the primary tumor location to a different location in the body through blood vessels and the lymphatic system during metastasis [3,4]. This invasion of new organs is responsible for approximately 90% of cancer deaths [5,6].

Cancer drug development is a complicated process that involves several costly and time-consuming steps. For a drug compound to be developed and reach the market, it takes between 10 and 15 years at a total estimated cost of US\$800 million [7]. The drug development process includes drug discovery, preclinical tests, and clinical trials. Preclinical tests include the performance of *in vitro* and *in vivo* tests, where the potential adverse effects of the cytotoxic drugs are investigated before initiation of clinical trials in humans [8]. This complex process shows that more-robust and faster methods to screen and validate potential drug candidates are urgently needed to provide an efficient improvement and cost reduction to the drug discovery process [9,10]. *In vivo* tests are performed in animal models, such as mice. In addition to ethical issues, animal models fail to mimic the human tumor physiology and it is known that the translation of successful results obtained with animal models to human clinical trials is <8% [11]. *In vitro* platforms can be used to study a variety of biological and physiological processes. However, conventional *in vitro* platforms are based on a 2D monolayer of cells and, consequently, fail to mimic the environment of the tissue [11,12] owing to the static conditions, the lack of a 3D microenvironment, and the absence of mechanical and/or chemical stimuli [11,13–15].

With the advent of microfluidics technology, novel culturing platforms have emerged that can be continuously perfused and imitate the physiological functions of tissues and organs [16]. Microfluidics studies the transport and manipulation of microliter and nanoliter volumes in channels as small as one human hair [17]. Microfluidic technology is based on the field of biological microelectromechanical systems (bioMEMS) and has been used in chemistry, pharmaceutical, biological, and medical research. Microfluidic devices provide a more realistic *in vitro* environment for the cells with the advantage of using small reagent volumes (microliters) [11,17]. Microfluidic platforms can generate mechanical stimuli, such as fluid shear stress, cyclic strain, and compression [16] in addition to a well-controlled concentration gradient of molecules [13,14]. All these characteristics make microfluidics a promising tool for the selection of potential anticancer drug candidates during screening processes. Here, we review *in vitro* cancer studies and the applications of microfluidic technology on anticancer drug development with a focus on: (i) the role of the tumor microenvironment in drug transport and metabolism; (ii) high-throughput assays for drug screening; and (iii) integrated biosensing platforms with the ability to monitor in real-time the dynamics of the tumor microenvironment. We summarize the advantages and disadvantages of the existing technologies and discuss future challenges toward the clinical translation of these technologies.

Tumor microenvironment

The tumor microenvironment is complex and plays an important part in the growth, invasion, and metastasis of cancers [18]. The environment of a normal tissue is extremely altered in the

presence of a tumor. The invasion and proliferation of cells in the tumor can reorganize the extracellular matrix (ECM) of the tissue, increase interstitial pressure, and create hypoxic regions within the cells [19] (Fig. 1). The ECM mainly comprises biomolecules such as proteins, polysaccharides, and water, and it is responsible for providing a physical scaffold for cells, containing biochemical and biomechanical cues that can direct cellular differentiation and homeostasis [20].

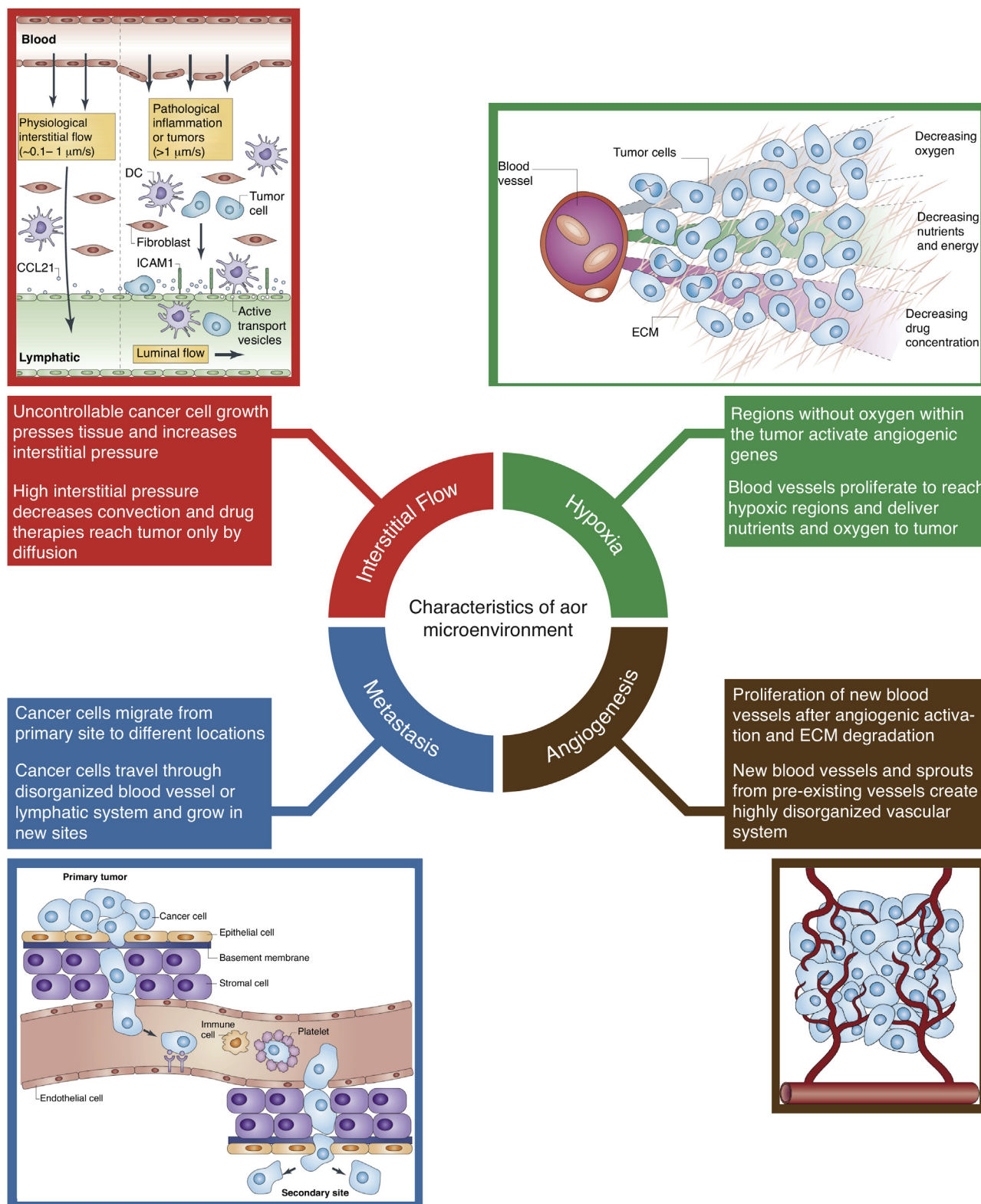
In addition to waste products, the degradation of protein components, such as collagen and fibronectin, also occurs inside the tissue [17]. This protein deposition creates stiffening of the ECM and is a diagnostic indicator of solid cancer [21]. A deregulated and abnormal ECM can also influence the behavior of endothelial cells, having an important role in tumor angiogenesis [22]. Moreover, the structure of the vascular network in tumors is highly disorganized, displays unusual leakiness, and expresses surface molecules that mediate the diffusion of tumor cells in the bloodstream and preserve the tumor microenvironment [23]. Such abnormalities in the tumor tissue result in the resistance of tumor cells to therapeutic agents and affect the transport of drug within the tumor [24].

Effect of hypoxia and interstitial pressure on drug penetration

One of the most well-known hallmarks of cancer is uncontrollable growth and multiplication of cancer cells [25]. Given that this growth occurs within a healthy tissue, the cancer cells develop a 'stressful' environment by pressing the cancer on the surrounding tissue and ECM. Elastic stress increases on this tissue, which can in return result in an increase in the intratumoral pressure [26]. The increase in pressure creates an interstitial fluid flow from the tumor to the surrounding healthy tissue, draining tissue lymphatics [19,24,26–28]. A poorly organized vascularization system combined with the rapid proliferation of cancer cells increases the amount of toxins and biomolecules, contributing to a rise in pressure in the tissue. The disorganized vasculature inhibits the distribution of large molecules by convection [26,28–30]. Therefore, within solid tumors, it is common to see the presence of hypoxic regions [19]. In these hypoxic regions, cancer cells use oxidative pathways to metabolize and produce more lactic acid and carbonic acid [31]. Consequently, the increase in interstitial pressure does not allow a good clearance of waste products and alters the pH within the tumor [28].

Hypoxia

Hypoxic regions are present in most tumors and increase the resistance of the cancer to therapeutic treatments [19,24]. In the case of systemic therapy, cytotoxic drugs are delivered to damage fast-growing cells. However, in many tumors, blood flows in a disorganized manner and, owing to excessive growth of cancer cells, blood vessels are not capable of reaching every part of the tumor, generating hypoxic regions where no oxygen, nutrients, or cytotoxic drugs can be delivered to the cells [19,24,28]. Consequently, hypoxic regions are often close to necrotic regions and create therapeutic resistance [28,32]. However, to survive, tumor hypoxia activates genes associated with angiogenesis in cancer cells [32] by secreting angiogenic activators, such as vascular endothelial growth factor (VEGF) and basic fibroblast growth factor (bFGF) [33–35]. These angiogenic factors stimulate the proliferation of blood vessels by sending a signal to induce new



Drug Discovery Today

FIGURE 1

Characteristics of the tumor microenvironment. Abnormal interstitial flow caused by pressure of cancer cells on tissue results in drainage of tissue lymphatics and decreases the efficacy of drug therapies. Hypoxia caused by absence of oxygen results in the activation of angiogenic genes. Angiogenesis resulting from the activation of angiogenic genes causes the proliferation of blood vessels and a disorganized blood network. Tumor metastasis results from the migration of cancer cells from the primary site to different tissues via intravasation into blood vessels and the lymphatic system. Reprinted, with permission, from [24,128–130]. Abbreviation: ECM, extracellular matrix.

endothelial cell growth and ECM degradation (matrix metalloproteinases) [33]. The degradation of the ECM allows endothelial cells to migrate and to start division, initiating blood vessel growth and sprouting from pre-existing blood vessels [33,34]. Once vascularized, the tumor is free to grow and metastasize to different regions of the body [36].

Interstitial pressure

Chemotherapeutic drugs can penetrate healthy tissues by diffusion and convection [24]. Whereas convection depends on a gradient of pressure between the blood vessel and the interstitial space, diffusion occurs as a result of a concentration gradient within the tissue. In healthy tissue, the interstitial fluid comprises an influx of nutrients and oxygen from blood vessels [26]. In the case of cancerous tissue, the interstitial fluid is poorly drained owing to the lack of lymphatic vasculature [24], resulting in an increase in interstitial pressure. Also, cancer cells invade a healthy tissue by pressing and pushing the surrounding environment, creating an increase in pressure inside the tumor and resulting in a large differential pressure between the tumor and the healthy tissue. Therefore, the drug penetration and distribution are limited to diffusion, decreasing the efficacy of systemic therapies [28].

Cytotoxicity studies in 2D and 3D *in vitro* cell cultures

Traditional drug studies are performed in 2D cultures, where cells are seeded on flat plates to form a monolayer. This method has been extensively used by researchers and pharmaceutical companies because of its simplicity. However, the translation of the results obtained from cancer cell monolayers to a tumor is not promising because 2D models are unable to replicate the cell–cell and cell–ECM signaling of complex 3D tissues [37]. For instance, in a 2D model, the cells are cultured on hard plastic substrates and exposed to uniform concentrations of nutrients and drugs in a static condition [38]. However, natural tumor cells reside in a 3D matrix with a disorganized network of blood vessels that distribute the bioactive molecules nonuniformly [39]. Therefore, great effort has been made during the past few years to develop more-reliable *in vitro* models by utilizing biomaterials and microfluidic technology [39]. 3D cell cultures allow the combination of multiple cell types and the presence of stromal matrix and ECM [40]. Moreover, the cell–cell and cell–ECM interactions combined with a 3D architecture create a closer functional resemblance to the *in vivo* tumor. In addition, 3D tumor models demonstrate less sensitivity to cytotoxic agents.

There are different methods used in the creation of 3D cell cultures. Spheroids have been widely used as cell culture systems for high-throughput cell culture in 3D. Spheroids can be formed using a forced-floating method where cells are deposited in a vessel and, after centrifugation, multicellular spheres are formed [41]. The hanging drop method can also be used in the creation of spheroids, where cells are suspended in a tray that is inverted, creating an agglomeration of cells [42]. Spheroid formation is also seen in agitation-based approaches, where cells are suspended in a container with a stirrer that promotes cell–cell interactions [43].

Pickl and Ries investigated the cytotoxic response of trastuzumab in human breast cancer (SKBR-3) and ovarian cancer (SKOV-3) cells cultured in 2D (monolayer) and in spheroids [44]. The efficacy of trastuzumab in the 2D culture was not promising, and it only slightly reduced cell proliferation. However, when the spher-

oids were treated with the drug, a proliferation inhibition of 48% was seen in the case of SKBR-3. To further investigate the origin of the successful results obtained when spheroids were treated with the anticancer drug, human epidermal growth factor receptor 2 (HER2) signaling was investigated in 2D and 3D culture models (Fig. 2a). Higher levels of phosphorylation of HER2 were induced in the spheroid formation. The results indicated that the difference in HER2 signaling seen in 2D and 3D cultures was due to a difference in the architectural phenotype of the culture system. The study emphasized the importance of closer *in vivo*-like cell culture models in the investigation of cell signaling and drug effectiveness.

The advantages of the use of spheroids over 2D cell cultures are numerous, such as the recapitulation of a 3D architecture of the tissue, including hypoxic regions on larger spheroids, and the possibility to recreate cell–cell and cell–matrix interactions [45]. Spheroids can also better mimic the response of the 3D tumor to cytotoxic treatments in terms of drug sensitivity and resistance [46]. However, even though the benefits of using spheroids are evident, there are still challenges to be overcome because spheroid culture is time-consuming, requires intensive labor, and may lack consistency in the production of uniform spheroid sizes [46].

Even though spheroids can mimic the 3D architecture of tumor and tissues, they still lack the presence of chemical and physical properties of the ECM. Bioengineered scaffolds have been extensively used for mimicking the complexities of the tumor microenvironment [47]. Scaffolds provide a 3D structural support to the cells and mimic physicochemical cues of the native tissue [48]. Scaffolds can be produced from naturally derived materials [49] or synthetic biomaterials [49,50] using biofabrication strategies including electrospinning [51], particle leaching [52], direct writing [53], and weaving [54]. The use of hydrogels as scaffolding materials has recently drawn much attention since they are 3D networks of polymeric materials that have a high water content and their physicochemical properties can be tuned to match the properties of the natural tissue [55,56].

Chen *et al.* investigated cellular properties, such as morphology proliferation and malignant phenotypes, of MCF-7 cells cultured in 3D collagen scaffolds [57]. MCF-7 cells cultured in collagen had a round and spread-out appearance, forming a multilayer structure in the scaffold. By contrast, 2D cell cultures displayed trigonal and polygonal shapes. In addition, secretion of proangiogenic growth factors, such as VEGF, bFGF, and interleukin (IL)-8, was more plentiful in 3D scaffolds than in the 2D cultures. Moreover, the quantity of cells presenting with a cancer stem cell-like CD44⁺/CD24^{-/low} phenotype (cell surface markers) in 3D was 34.1%, whereas only 3.5% of the cells in 2D presented the same markers. To study the tumorigenic capability of the 3D cultured cells, xenografts and scaffolds loaded with cells cultured in 2D were implanted in mice. After 5 weeks, the 3D cultured cells created a tumor weighing 0.7 ± 0.26 g, whereas the 2D-derived tumor was 0.17 ± 0.27 g (Fig. 2b). The results indicated the importance of the 3D scaffold in cell culture. The cells cultured in a 3D collagen scaffold created a better representation of the *in vivo* tumor, with overexpression of proangiogenic factors and higher tumorigenicity when implanted *in vivo*.

Material composition and physicochemical properties play an important role in cellular function and drug efficacy in 3D cul-

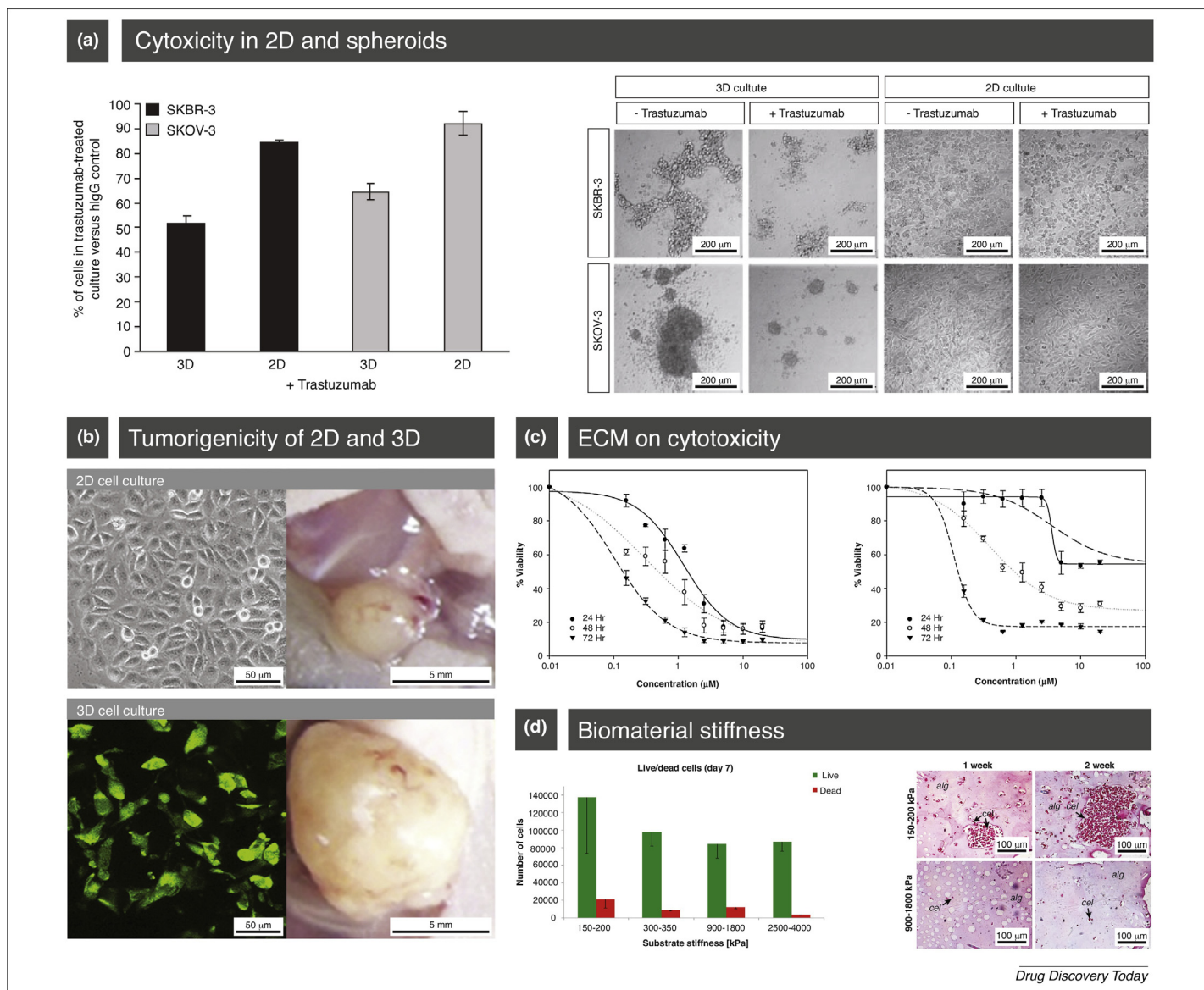


FIGURE 2

Drug cytotoxicity studies performed in 2D and 3D cell culture models. **(a)** Effect of trastuzumab on breast cancer cells (SKBR-3 and SKOV-3) cultured in 2D and 3D: cell viability (left) and phase-contrast micrographs (right). **(b)** Tumorigenicity of 2D monolayer of MCF-7 cell cultures (left) and of the tumors (right). **(c)** Cytotoxic response curves after 24 h, 48 h, and 72 h of exposure of HeLa cells on 2D (left) and 3D collagen (right) to doxorubicin. **(d)** Effect of matrix stiffness on viability of breast cancer cells (MCF-7) (left) and cluster formation on soft (150–200 kPa) and stiff (900–1800 kPa) alginate hydrogels (right). Reprinted, with permission, from [44] (a), [57] (b), [58] (c), and [59] (d).

tures. In an interesting study by Casey *et al.*, the impact of the ECM on the toxicity of doxorubicin (DOX) on human cervical (HeLa) cells was analyzed in 2D and in 3D collagen matrices [58]. The results showed that the drug was less efficient in the 3D cell matrix compared to the 2D monolayers in the first 24 h. This reduction in the cytotoxicity was attributed to the interaction of the drug and the collagen matrix. However, after 72 h, no significant difference was observed in cell viability between 2D and 3D cultures (Fig. 2c). The outcomes of this study showed the importance of the matrix composition on drug efficacy.

The importance of selecting the appropriate biomaterial during the development of a 3D *in vitro* model was also investigated by Cavo *et al.* [59]. Breast adenocarcinoma MCF-7 cell activity was evaluated after seeding the cells in 3D alginate gels, with alginate

and calcium chloride concentrations ranging from 0.5% to 2% and 0.5 M to 1 M, respectively. Cell viability results showed that the amount of live cells was influenced by the stiffness of the substrate. The number of live cells was high in gels with low elastic modulus (i.e., 150–200 kPa, 300–350 kPa, and 900–1800 kPa). To investigate cell cluster formation, MCF-7 cells were seeded in the low-elastic gels. The results showed that cells inside the 150–200-kPa alginate hydrogels formed 300- μ m spheroids after 14 days, whereas only a few cells formed clusters in stiffer gels (Fig. 2d). The results of this study indicated that matrix stiffness can affect the diffusion of nutrients and intracellular signaling.

Compared with spheroids, scaffolds combine properties of the ECM to better recapitulate *in vivo* cell–ECM interactions. The presence of a scaffold not only provides structural support to

encapsulated cells, but can also affect cell behavior and function [8]. However, there are still limitations to the use of bioengineered scaffolds. Synthetic, natural, or a combination of both, the material used in the construction of a scaffold needs not only to be compatible, but also to match the mechanical properties seen in the natural tissue [60]. The matching of stiffness, elasticity, porosity, and biodegradability rate can be challenging for highly complex tissues and can require the combination of more-sophisticated and -complex biomaterials.

Although 3D cell culture models present many advantages compared with 2D cell monolayers, 3D cell cultures still do not mimic relevant key aspects of *in vivo* tissues [61]. 3D *in vitro* cell cultures fail to reproduce a dynamic environment, where interactions and communications between different cell cultures are seen in the presence of fluid flow perfusion [62,63]. Microfluidic technology was applied to bioengineering research to overcome the limitations seen in current 3D cell culture models. Microfluidic devices allow the creation of an *in vitro* tumor environment that closer resembles the *in vivo* situation because of precise spatial and temporal control of nutrients, oxygen, and cytotoxic drug delivery [38] and integrated biochemical and mechanical features [62]. In addition to providing a more realistic *in vitro* environment for small-scale systems, microfluidic devices are cost efficient since they require small sample and reagent volumes, are transparent, and can be used to perform high-throughput assays [64] (Table 1).

Microfluidic technologies

Microfluidic platforms have recently emerged as powerful tools for recreating the complexities of the natural tissues and disease modeling [65,66]. Owing to their small dimensions, laminar flow is seen inside the channels and viscous forces dominate over inertial forces [62]. Mass transport of nutrients and gases inside microfluidic devices occurs by diffusion, which closer mimics the *in vivo* delivery of nutrients. The small dimensions of the channels allow precise control of the system and a low volume of reagents, which, consequently, reduces equipment and sample costs. In addition, the small dimensions are comparable to the dimensions encountered inside the human body, allowing better replication of human tissues *in vitro*. Microfabrication techniques have been used in the development of microfluidic devices, including soft lithography and replica molding, injection molding, and 3D printing [67]. Among different materials, poly(dimethylsiloxane)

(PDMS) is the most common material used in microfabrication. PDMS is a transparent biocompatible silicon-based polymer that allows high gas permeability, providing sufficient oxygen permeation to cell culture systems [62]. Microfabrication techniques present enough flexibility to develop different designs of microfluidic devices. Therefore, the addition of a chemical gradient generator combined to sensing technology and mechanical stimuli allows the development of predictive platforms of human physiology and disease for drug development [16]. Table 2 lists the advantages of microfluidic devices over traditional 2D and 3D *in vitro* cell culture models.

Modeling the tumor microenvironment

Microfluidic devices have been extensively used in cancer research. Owing to the high flexibility of architectural design fabrication, different types of cancer models can be developed in microfluidic platforms. Most cancer-on-a-chip models are breast, lung, and liver cancers because of their high incidence rates [1]. Breast cancer is still one of the most lethal types of cancer, responsible for more than 40 000 estimated deaths in the USA alone in 2016 [1]. Therefore, much effort has been made to develop microfluidic-based breast cancer models and investigate the cancer progression and efficacy of different drugs. For instance, a multi-channel microfluidic device was developed to investigate the crosstalk of breast cancer cells and immune cells [68]. In this study, MD-MB-231 breast cancer cells were suspended in collagen and injected in two channels of the microfluidic device (Fig. 3a). Macrophages were then suspended in Matrigel™ and injected in the central channel between the two breast cancer collagen channels. The co-culture was incubated for over 1 week and no movement was seen in the breast cancer culture toward the Matrigel™ layer. By contrast, the macrophages had migrated and invaded the collagen cancer cells by day 3. This invasive behavior was more extensively seen after 7 days, when macrophages also showed an increase in number because of their multiplication in presence of MDA-MB-231 cells. The results of this study proved the ability of microfluidic platforms to mimic the crosstalk between the cancer cells and the immune cells.

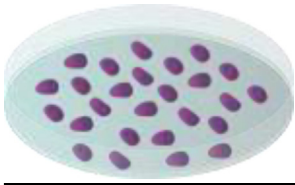
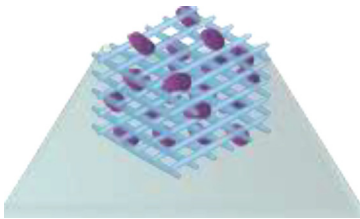

Ductal carcinoma *in situ* (DCIS) is a type of noninvasive breast cancer that occurs inside the milk duct. However, some of these cancer cells have the ability to migrate from the original duct region to the surrounding tissue (invasive ductal carcinoma). A

TABLE 1
Summary of 2D and 3D *in vitro* cell culture models

Study	2D	3D	Refs
Cytotoxic response of trastuzumab in breast cancer (SKBR-3) and ovarian cancer (SKOV-3) in 2D and 3D <i>in vitro</i> models	Trastuzumab only slightly reduced cell proliferation in the monolayers (~10% inhibition)	48% proliferation inhibition seen for SKBR-3 and ~35% inhibition for SKOV-3	[44]
Study of tumorigenic capability of breast cancer cells (MCF-7) cultured in 2D and 3D models	2D-derived tumor implanted into mice and, after 5 weeks, resulted in a tumor weighing 0.17 ± 0.27 g	3D-derived tumor implanted in mice created a tumor weighing 0.7 ± 0.26 g after same 5 weeks	[57]
Impact of ECM on therapeutic effect of doxorubicin on human cervical (HeLa) cells cultured in 2D and 3D collagen matrices	After 24 h of exposure to doxorubicin, toxic effect of drug in 2D cell culture generated $IC_{50} = 1.2 \pm 0.3$ μ M	Effect of doxorubicin in 3D cell models was lower than in 2D cultures, with $IC_{50} = 3.6 \pm 1.33$ μ M	[58]
Effect of matrix stiffness on breast cancer cells (MCF-7)	Cells cultured in a petri dish showed a flat shape	3D-cultured cells maintained a circular shape, forming 300- μ M spheroid clusters in less stiff alginate matrices	[59]

TABLE 2

Advantages and disadvantages of *in vitro* cell culture models

Culture model	Advantages	Disadvantages
2D cell culture 	Methodology well established Simplicity to work with cell monolayer	Static conditions Uniform concentration of nutrients and drugs Lack of 3D environment Large reagent volumes
3D cell culture 	Cell-cell and cell-ECM interactions Sensitivity to cytotoxic agents similar to <i>in vivo</i>	Failure to produce dynamic environment Lack of fluid flow perfusion
Microfluidic platforms 	Higher control of environment Diffusion of nutrients and drugs Cost-effective Combination of CGG, biosensors, and mechanical stimuli High-throughput assays	Nonstandardized protocols PDMS can adsorb molecules Perfusion of more than one growth medium can be challenging

microfluidic platform to replicate DCIS in a 3D *in vitro* model was developed comprising upper and lower channels separated by a collagen membrane (Fig. 3b) [69]. The lower channel recreated the stromal tissue in the mammary duct by seeding cancer-associated fibroblasts on a collagen-coated membrane. By contrast, endothelial cells were cultured in the presence of a mixture of MatrigelTM and fibronectin on top of the collagen membrane. The culture of different cell types was possible in the DCIS-on-a-chip model owing to the presence of two chambers, where different types of growth medium were delivering nutrients to the cell cultures. DCIS spheroids were allowed to adhere to the epithelial layer on the top channel. Cytotoxic evaluation of anticancer drug paclitaxel (20 nM) was performed by injecting the drug on the lower channel (stromal-like culture) for 24 h to simulate an intravenous administration of the drug. Lactate dehydrogenase (LDH) levels released from the epithelial cells and fibroblast were used to assess drug cytotoxicity. The results indicated that production of LDH doubled at day 4 when DCIS spheroids were present in the upper channel. However, in the case of the control experiments performed on the chip in presence of a monolayer of epithelial cells, no change in cytotoxicity was seen. Spheroid sizes inside the microfluidic device in the presence and in the absence of the anticancer drug were compared and the results indicated the efficacy of paclitaxel. Untreated spheroids were nearly threefold the size of the treated spheroids. The results indicated the importance of developing a 3D architecture and microenvironment to assess cytotoxicity of cancer drugs.

Cancer can become even more complex to treat when it migrates from its original place to different tissues inside the body.

Tumor extravasation is known as metastasis and it has been largely explored using microfluidic systems. The extravasation of breast cancer cells to bone was studied using a 3D microfluidic model [70]. The microfluidic platform comprised eight gel channels and three media channels and was previously used to investigate angiogenesis [71–73]. A triculture system was generated by the injection of human osteo-differentiated bone marrow-derived mesenchymal stem cells embedded in a collagen matrix in one of the channels, whereas endothelial cells were seeded in the central channel to create an endothelial cell barrier covering the lateral wall of the channels. Breast cancer MDA-MB-231 cells were introduced in the endothelial channel (Fig. 3c). The results demonstrated that the cancer cells migrated through the collagen layer by penetrating the endothelial barrier. This migration was also confirmed in the absence for osteo-differentiated bone cells. However, in presence of these cells, 77.5% of cells migrated to the bone matrix, compared with only a 38% extravasation rate seen when pure collagen was present. To further study the role of the osteo-differentiated bone cells in the extravasation of breast cancer cells, the expression of chemokine CXCL5 was investigated in the bone compartment. This specific chemokine is known to be involved in cancer migration by expression of surface receptor CXCR2 [74]. The production of CXCL5 by the bone cells was confirmed and the expression of CXCR2 surface receptor was shown to be present in cancer cells. After blocking the CXCR2 receptor, the rate of cancer cell extravasation decreased from 77.5% to 45.8%. This study elucidated the use of a microfluidic system to study cancer metastasis, where different cell lines could be cultured inside a chip.

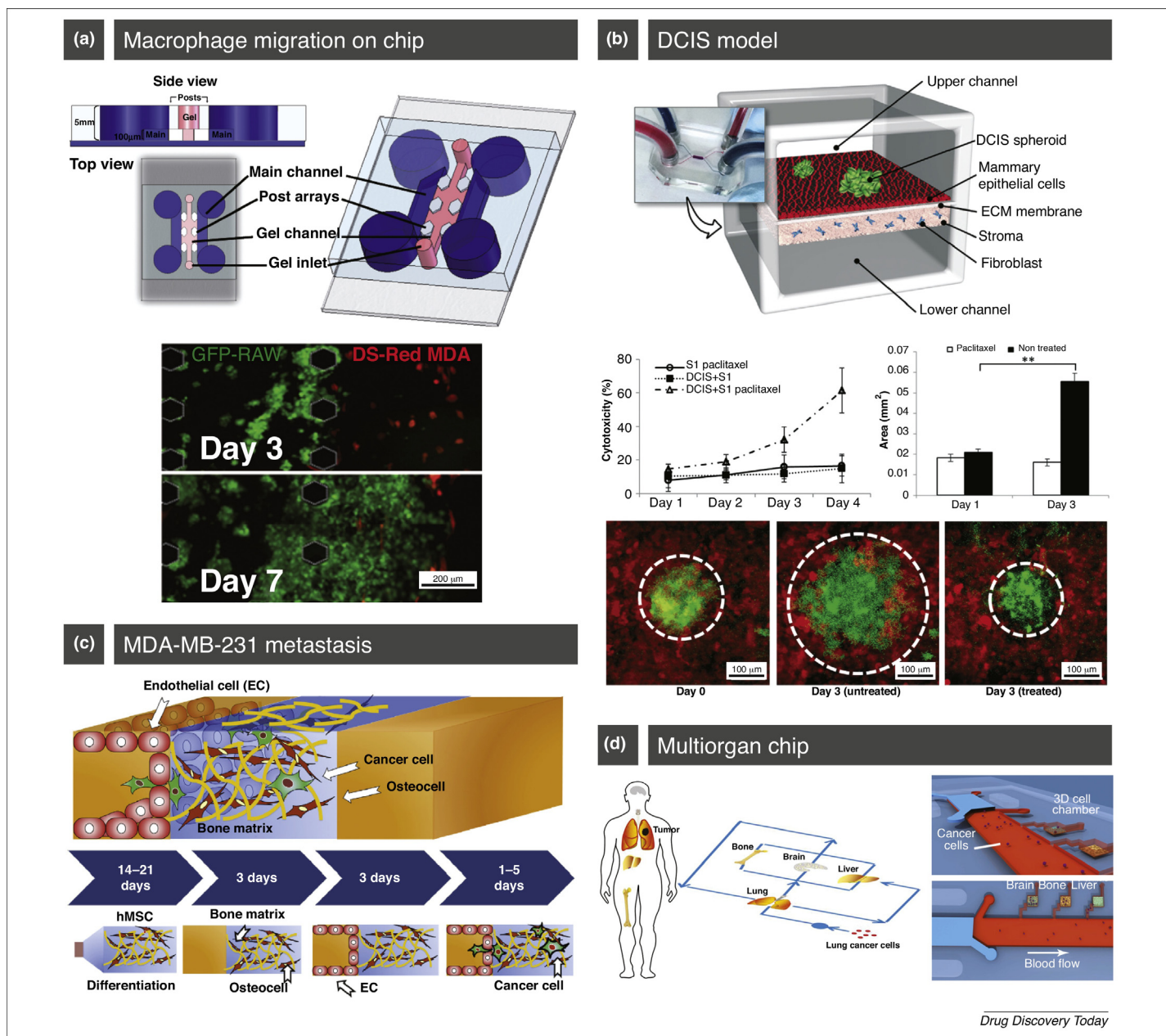


FIGURE 3

Biomimetic *in vitro* cancer models. **(a)** Microfluidic device for cell co-cultures in different matrices: design of the chip (top) and migration of macrophages (in green) toward tumor cells (in red) suspended in Matrigel™ (bottom). **(b)** Microfluidic platform to mimic the microarchitecture of ductal carcinoma *in situ* (top) composed of upper and lower cell channels separated by an extracellular matrix (ECM)-derived membrane. Cancer spheroids were embedded in the mammary epithelial layer on the upper channel, where a fibroblast-containing stromal layer was formed in the lower chamber. The effect of paclitaxel in the breast tumor-on-a-chip (bottom) is illustrated by fluorescence micrographs of the spheroid sizes (shown in green) in absence and in presence of the cytotoxic drug. **(c)** 3D microfluidic device for MDA-MB-231 breast cancer cell extravasation to bone: generation of the osteo-cell-conditioned microenvironment, where endothelial cells were cultured to create a barrier covering the lateral wall of the microchannels and breast cancer cells were seen to migrate toward the differentiated bone cells through the endothelial layer. **(d)** Biomimetic multiorgan microfluidic chip system composed of lung, brain, bone, and liver for the study of metastasis of lung cancer cells to 'distant organs'. Reprinted, with permission, from [68] (a), [69] (b), [70] (c), and [75] (d). Abbreviation: hMSC, human mesenchymal stem cells.

Lung cancer is one of the leading causes of death as a result of cancer and was responsible for 27% of all cancer deaths in 2016 in the USA [1]. The high mortality rate occurs because symptoms of lung cancer are difficult to distinguish from normal infections or disorders arising from side effects of smoking. Therefore, lung cancer is generally diagnosed in its advanced stages. Lung cancer metastasis was studied in a multiorgan microfluidic device

comprising a lung and three 'distant organs': brain, bone, and liver (Fig. 3d) [75]. Lung cancer A549 cells cultured inside the microfluidic device formed a cancer mass, showing epithelial mesenchymal transition (EMT), whereas the level of EMT markers (E-cadherin, N-cadherin, Snail 1, and Snail 2) were used to evaluate the invasion of A549 cells to the distant organs. In addition, the formation of a tumor mass in the brain, bone, and liver was

analyzed by mesenchymal–epithelial transition (MET) markers. Thus, the expression of the markers in A549 cells in distant organs indicated that the lung cancer cells had metastasized from the primary site to the different organs in the microfluidic device. This invasive capability could only be analyzed owing to the integration of multiorgans-on-a-chip, promoting the investigation of cell–cell interactions during the process of metastasis.

Microfluidic devices present many advantages over conventional 2D and 3D cell culture models, including high spatial and temporal control of the system, the use of low sample volumes, and the ability to incorporate mechanical and chemical features in the platforms. However, there are still a few challenges to be overcome. For instance, most microfluidic devices are developed for specific applications and, consequently, there is a lack of translation from one type of cancer to another using the same platform. In addition, the integration of different types of biochemical factors to recapitulate a more complex tumor microenvironment remains a challenge [76]. Limitations can also be seen in the extraction of data from microfluidic devices: most results can only be obtained using microscopy, whereas a large amount of information in terms of the molecular level is lost [77].

High-throughput assays for drug discovery

The drug discovery process requires the analysis of thousands of drugs before preclinical trials. To assess the efficacy of this large number of compounds, high-throughput screening (HTS) platforms are used in target discovery. Given that microfluidics requires a low amount of reagent (cost-effective) and allows parallel processing (less time-consuming), microfluidic platforms are an attractive option for high-throughput assays. To measure the cellular response of liver carcinoma cells (HepG2), Ye *et al.* developed a microfluidic platform comprising a concentration gradient generator (CGG) connected to cell culture chambers, in which liver carcinoma cells were seeded [78]. The entire microfluidic platform comprised eight microfluidic devices connected by a central common reservoir (Fig. 4a). The presence of a CGG allowed the characterization of cytotoxic effects on the cells in culture using different concentrations of anticancer drugs. Cytotoxic effects of different drugs, including actinomycin and daunorubicin, in the hepatocyte culture were assessed using the platform, where selectivity in inducing apoptosis in the HepG2 cells was detected. Characterization of intracellular redox states, including reactive oxygen species and reduced glutathione, in the cells enabled correlation of the selective effects of the anticancer drugs with cell oxidative stress by using fluorescence probes inside the platform, providing an easy and rapid method to measure cellular response [78].

Similarly, Xu *et al.* combined a CGG in a microfluidic platform to test drug sensitivity in the treatment of lung cancer [79]. The platform comprised a CGG, for cytotoxic drug input, connected to cell culture chambers (Fig. 4b). Co-culture of human lung fibroblast cells (HFL1) and human non-small cell lung cancer cells (SPCA-1) were suspended in a Cultrex[®] basement membrane extract and added to the cell culture chambers. Lateral perfusion channels delivered cell medium to the co-culture. The microfluidic chip was used to test the toxicity of several anticancer drugs, including gefitinib (0.8125 μM), paclitaxel (8.125 μM),

gemcitabine (162.5 μM), and cisplatin (16.25 μM). Different chemotherapy schemes were investigated by combining two different drugs in the CGG: paclitaxel and cisplatin. IC₅₀ values demonstrated the effect of the drugs on cancer cell growth. Combined chemotherapy schemes showed that the combination of paclitaxel and cisplatin was more effective (higher rate of apoptosis) than the treatment of paclitaxel alone. Higher resistance to apoptosis was seen in the co-culture compared with drug sensitivity studies performed in the lung cancer cell line alone, demonstrating the impact of stromal cells on drug cytotoxicity. The microfluidic platform was also used to test drug sensitivity in a co-culture of cancer cells and stromal cells obtained from fresh lung cancer tissues of eight patients undergoing surgical resection for lung cancer. Drug sensitivity studies demonstrated that the results obtained were similar to those obtained with the cells lines. However, IC₅₀ values indicated higher sensitivity in the patient cancer cells than in the cultured cancer cell lines. In addition, different IC₅₀ values were obtained for different patient samples, showing that the stage of lung cancer had a big impact on drug efficacy. Nevertheless, the microfluidic device provided a high-throughput platform for drug sensitivity tests and the potential for the inclusion of the platform as a routine clinical test to design individualized lung cancer treatments.

Combinatorial drug therapies for cancer treatment have been studied for a long time [80–82]. However, the assessment of numerous combinations of chemotherapy drugs in 2D cell cultures is time-consuming and unrealistic when compared to the 3D microenvironment of the human body. Ding *et al.* developed a microfluidic print-to-screen platform to assess drug cytotoxicity (Fig. 4c) [83]. The platform uses a microfluidic impact printer comprising different microfluidic channels that allow the printing of various biological reagent droplets on top of a substrate. The HTS of combinatorial chemotherapy drugs is performed by printing multiple drug-containing droplets in a specific target spot. The effect of ten anticancer drugs, including tamoxifen, thalidomide, and celecoxib, was evaluated by printing these drugs on top of a pre-patterned agarose gel array located on a PDMS substrate. The hydrophilic spots of the agarose gel worked as an anchor for the printed droplets. Ovarian cancer cells (SKOV-3) were mixed with agarose hydrogel solution and allowed to perform gelation to form a cell-embedded soft agarose gel sheet. The sheet was then deposited on top of the printed array containing combinatorial chemotherapy drugs. Cell viability was assessed by quantifying the intensity level of fluorescence obtained when using a LIVE/DEAD assay. The cytotoxic effects of the anticancer drugs were labeled with a three-level color coding, where red indicated the highest cytotoxic effect (>47% cell were killed), yellow represented intermediate effect (42–47% cells killed) and green showed low cytotoxicity (<42% killed). The results indicated that, from the 165 different drug combinations used, only 15 showed high cytotoxicity effect (red color code) resulting from the combination of three drugs. The conclusions obtained from this study were pioneering in the field of treatment for ovarian cancer, where there was no previous report of a combination of three cytotoxic drugs in the treatment of this type of cancer. In addition, the high-throughput platform allowed for the low-cost and highly effective screening of combinatorial drugs and the time-effective performance of 165 assays.

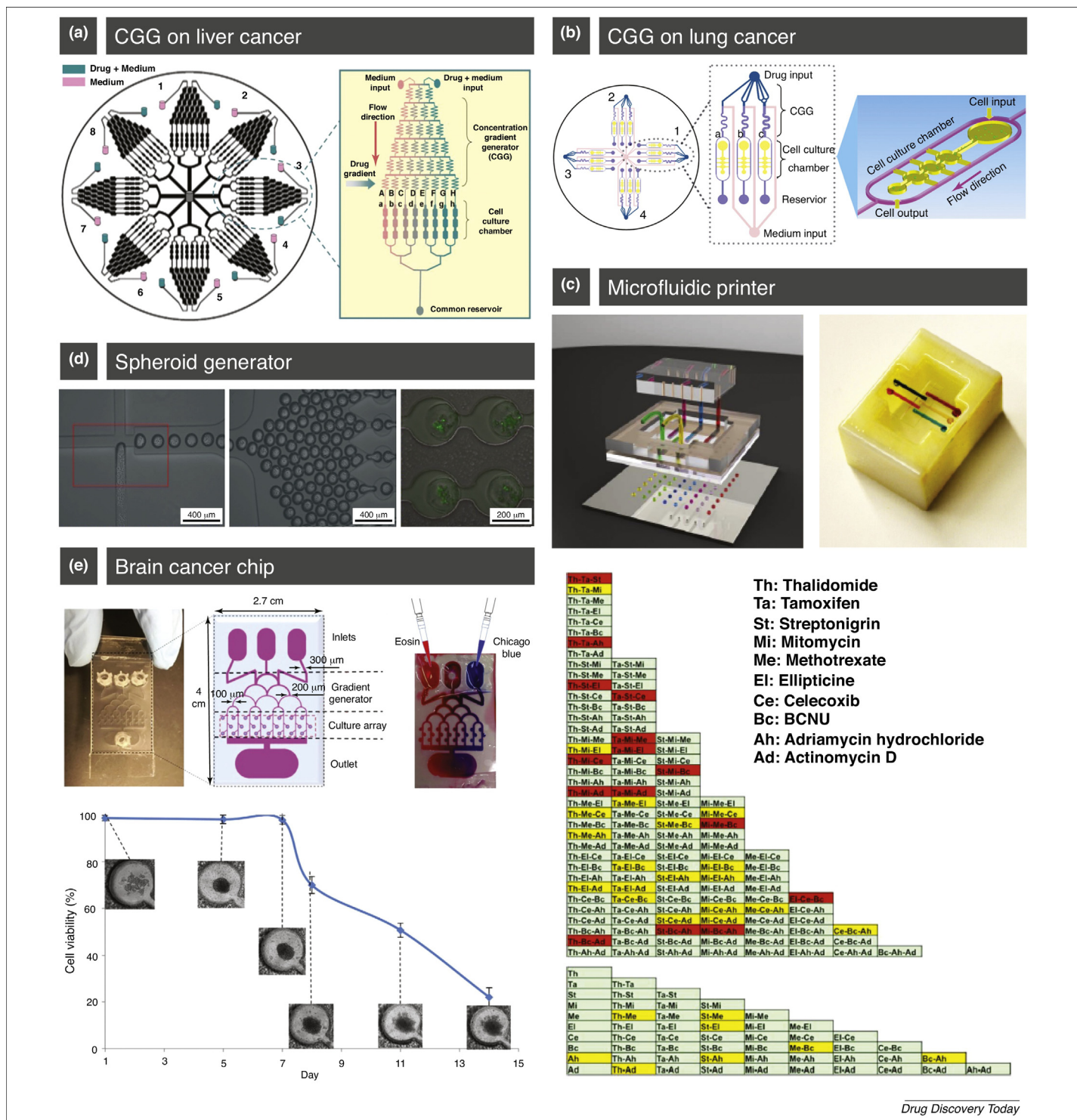


FIGURE 4 High-throughput microfluidic assays. **(a)** High-content screening microfluidic device composed of a concentration gradient generator (CGG) for measurements of cellular response of liver carcinoma. **(b)** A lung-cancer-on-a-chip integrated microfluidic device composed of cell culture chambers and CGG. **(c)** Microfluidic impact printer composed of microfluidic channels that allow the printing of droplets on top of a substrate (top). The high-throughput platform allowed the performance of 165 drug toxicity assays (bottom). **(d)** Spheroid generator using a droplet-based microfluidic device (left and middle). Live cells in spheroids were labeled in green (right). **(e)** High-throughput brain cancer microfluidic device composed of poly(ethylene) glycol diacrylate (PEGDA) channels (left and middle). The chip was composed of a CGG connected to multiple cell microwells. Combinatorial screening of dyes shows the CGG (right). Cell viability of U87 cells in a microwell during application of cytotoxic drugs on day 7 (bottom). Drugs released from the hydrogel layer affected cancer spheroids. Reprinted, with permission, from [78] (a), [79] (b), [83] (c), [84] (d), and [90] (e).

It is known that, although 2D cell monolayers are easy to handle, they fail to mimic the complexity seen in tumors. 3D cellular models, such as spheroids, have been used to demonstrate higher drug resistance compared with 2D monolayers. An integrated high-throughput microfluidic droplet assay was developed to generate multicellular spheroids (Fig. 4d) [84]. In addition to the generation and entrapment of over 1000 multicellular spheroids, the platform also allowed for the sequential analysis of the produced spheroids. The device comprised three different inlets for cells, oil, and calcium, and 1000 droplets docking sites. Spheroid droplets were formed in a T junction, where cells encapsulated in alginate droplets underwent gelation when in contact with calcium chloride solution. Co-culture spheroids were formed by adding a second inlet to the microfluidic platform, where the addition of MCF-7 breast cancer cells (MCF-7S wild type and MCF-7R resistance type) and bone marrow stromal fibroblast line (HS-5) was performed. To validate the results obtained with the spheroids, control experiments were performed in a 96-well plate. Cytotoxicity assays using two anticancer drugs [DOX (0.8–12.8 μM) and paclitaxel (12.8 μM)] were assessed in the microfluidic platform and the results were compared with a 2D monolayer. The results illustrated the benefits of using a 3D cell architecture to mimic a tumor: the MCF-7R cell viability obtained when using the highest concentration of DOX was 90% in spheroids and only 60% in the monolayer. For the MCF-7S cells, the results were significantly distinct, where approximately 70% of the cells were alive in the spheroids and only approximately 25% of the cells had survived in the monolayer after treatment with the highest concentration of DOX. Given that the cytotoxicity results of both MCF-7 cell lines were similar, the 3D architecture can be associated with high drug resistivity. The effect of anticancer drugs was also evaluated in a co-culture formed by MCF-7S cells and fibroblasts. As expected, the cell viability was higher when fibroblasts were present in the spheroids for the sample drug concentration. Combinatorial drug screening was assessed by administering DOX and paclitaxel simultaneously. There was a 12% decrease in cell viability when the combined therapy was used, compared with DOX alone. Therefore, the microfluidic device was not only capable of developing multicellular spheroids, but also had the

ability to perform a drug cytotoxicity assay in the spheroids on the same platform [84].

Conventional microfluidic devices are fabricated using photolithography techniques to create a patterned mold. PDMS is a transparent silicon-based polymer that is used in the fabrication of most microfluidic devices. However, although PDMS presents many advantages, such as optical transparency, flexibility, biocompatibility, and gas permeability [85,86], it is also known to adsorb small hydrophilic molecules, such as proteins, which can alter pharmacological activity results [87–89]. Fan *et al.* developed a high-throughput drug screening microfluidic device that mimicked brain cancer (Fig. 4e) [90]. The microfluidic channels were not fabricated using conventional PDMS but instead comprised poly(ethylene) glycol diacrylate (PEGDA) hydrogel that was patterned by using a photomask under ultraviolet (UV) light. After UV light exposure, a hydrogel microfluidic device was fabricated containing three inlets connected to a CGG. The outlets of the CGG were connected to 24 individual culture chambers. To capture the cells in the cell culture chambers, glioblastoma cells (U87) were diluted with cell medium and injected into the inlet of the device. After diffusion throughout the PEGDA channels, cells were captured in circular chambers and extra cells in the microchannels were removed by the addition of fresh medium. The cells inside the culture chambers formed spheroids after culturing for 7 days. High-throughput drug screening experiments were performed by injecting the anticancer drugs pitavastatin and irinotecan into each inlet port. Cell viability results demonstrated that cells started to detach from the spheroids and undergo cell death after receiving the anticancer drugs by diffusion. In addition to demonstrating an efficient high-throughput platform for drug screening in brain cancer cells, Fan *et al.* also illustrated a promising substitute for PDMS in microfluidic applications [90].

As discussed above, microfluidic devices provide the opportunity to develop high-throughput platforms for anticancer drug studies. However, in most chips, there is still a lack of sensing recognition elements to provide real-time detection. Therefore, the integration of biosensor technology in microfluidics allows the creation of powerful tools with biological and chemical components present in a single device [91] (Table 3).

TABLE 3

Summary of microfluidic devices

Cancer	Biomarkers	Refs
Breast cancer (MDA-MB-231)	Macrophage migration toward cancer cell chamber showed crosstalk between cancer and immune system	[68]
Breast cancer (MCF-10)	Cytotoxic evaluation of paclitaxel in DCIS spheroids seeded on epithelial cell layer. Chemotherapeutic drug was administered through fibroblast-containing stromal layer to reach tumor	[69]
Breast cancer (MDA-MB-231)	Investigation of metastasis of breast cancer cells to bone through production of CXCL5 by bone cells and expression of CXCL2 by cancer cells	[70]
Lung cancer (A549)	On-chip analysis of A549 cell metastasis from lung to 'distant organs' composed of brain, bone, and liver via cell markers	[75]
Liver cancer (HepG2)	Cytotoxic evaluation of different drugs in HepG2 cells using a CGG for fast and high-content screening	[78]
Lung cancer (SPCA-1)	Fast and parallel cytotoxic evaluation of several anticancer drugs in lung cancer cells by presence of a CGG in microfluidic device	[79]
Ovarian cancer (SKOV-3)	HTS of combinatorial chemotherapy drugs by development of a microfluidic impact printer, allowing 165 fast and low-cost drug combination tests	[83]
Breast cancer (MCF-7)	On-chip production of cancer spheroids and performance of cytotoxic assays	[84]
Brain cancer (U87)	On-chip formation of spheroids and assessment of cytotoxic assays through presence of a CGG	[90]

Microfluidic-integrated biosensors for cancer drug studies

Application of biosensors to cancer research is an emerging field for the development of highly sensitive, rapid, reliable techniques for the accurate detection of cancer, monitoring the tumor microenvironment, and characterization of tumor–drug interactions. Traditional cancer screening methods are based on taking a biopsy and relying on cell staining and fixation using microscopic techniques to identify cancer cells and biomarkers [92]. However, because these types of test are invasive, further alternatives are required to identify the malignancy without invasive examinations. The presence of biomarkers transmitted from the tumor to body fluids (blood and urine) can be instrumental for the early detection of cancer and, consequently, increase the patient survival rate [93–95]. Cancer biomarkers are useful for early cancer detection, especially when compared with time-consuming techniques, such as Enzyme-linked Immunosorbent Assay (ELISA) and Polymerase Chain Reaction (PCR) [96]. Table 4 lists the known biomarkers for several types of cancer. Cancer-related protein biomarkers can exist at low concentrations (10^{-15} – 10^{-12} M) in biofluids, which makes them applicable for health monitoring and biological applications [97].

Many studies focus on the use of microfluidics for biosensing applications. The coupling of biosensors with microfluidics gives great benefits, including higher selectivity, miniaturization, small sample volumes, multiplexing, and faster screening time. The combination of biosensors with organ-on-a-chip platforms provides an integrated platform for monitoring the tumor microenvironment [98,99]. The ultimate goal of microfluidic biosensors is to achieve selective detections of a large number of biomarkers with minimal sample preparation or user involvement [100].

One of the changes observed in the tumor microenvironment is the high metabolic activity of the cancer cells that alter the consumption of oxygen and change pH of the tumor extracellular matrix [101]. An integrated microfluidic device was developed to detect oxygen concentration and its chemical gradient within high-throughput tumor models [102]. A gas-permeable membrane made of PDMS mixed with platinum octaethylporphyrin dye (PtOEP) was fabricated to measure oxygen consumption (Fig. 5a). Na_2SO_3 as an oxygen scavenger was mixed with the

culture media and flowed into microchannels while human lung adenocarcinoma A549 cells and human cervical carcinoma HeLa cells were cultured inside the microfluidic chip. Oxygen consumption was measured as the change in fluorescence before and after the injection of the anticancer drugs tirapazamine (TPZ) and bleomycin (BLM). Similar high-throughput oxygen biosensors were also developed by incorporating optical techniques relying on fluorescence-emitting polymeric nanoparticles [103–107] and electrochemical impedance spectroscopy [108]. Highly sensitive and tunable nanoparticles were also developed to gauge the change in the pH of the tumor cellular environment [109,110].

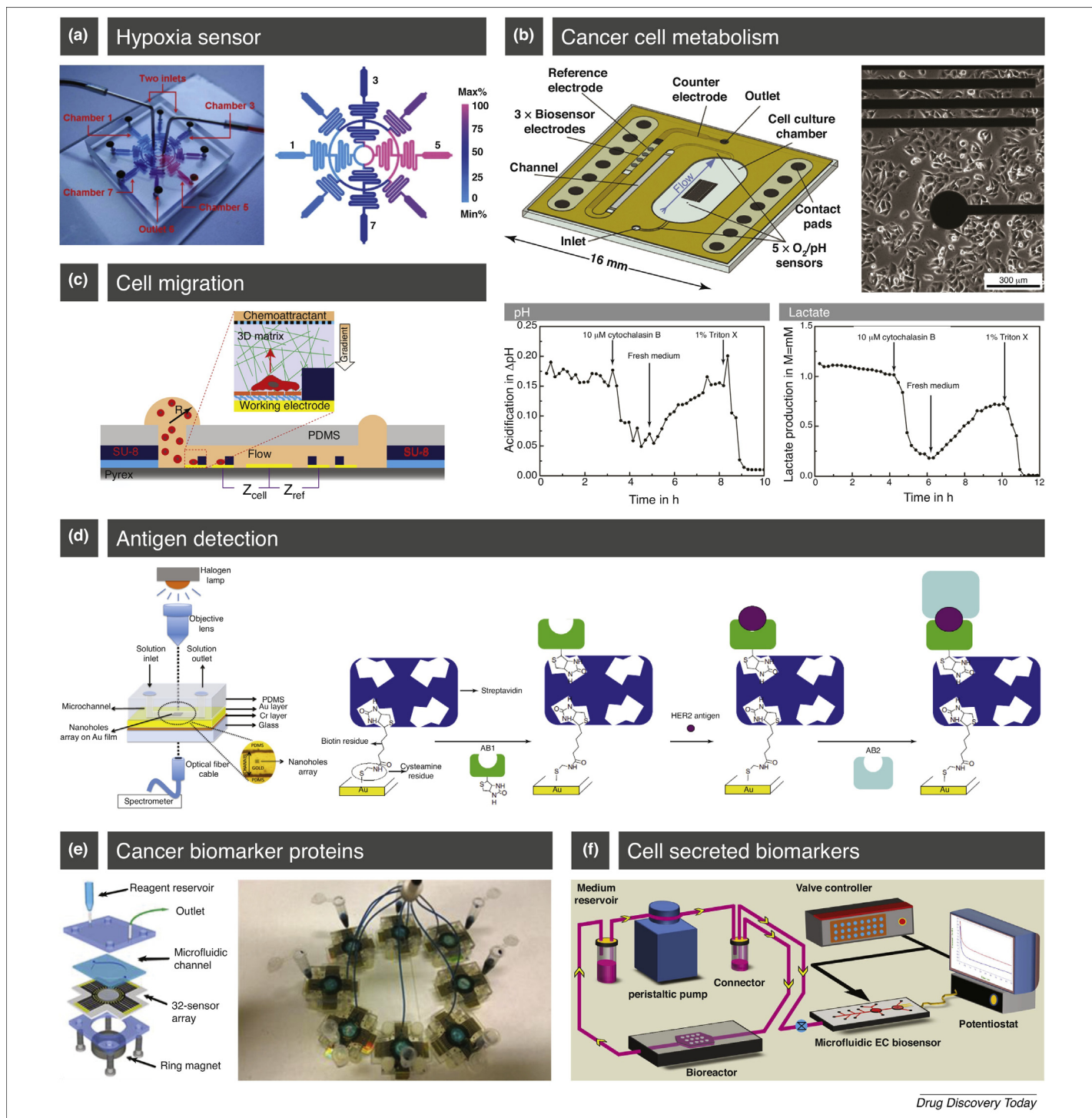
During the analysis of cellular metabolism, different parameters, such as pH and glucose uptake, are relevant. Weltin *et al.* developed a multisensor microsystem comprising a cell culture area, chemical sensors (pH and oxygen), and biosensors (lactate and glucose) integrated in a microfluidic platform (Fig. 5b) [111]. Human brain cancer cells were cultured in the cell culture chamber and the metabolism of these cells was measured on the chip. Glucose blocker cytochalasin B (CB) and detergent Triton™ X-100 were added to the cell medium to induce alteration in cellular metabolism. In terms of pH levels, a change from a stable acidification to a decrease in pH was seen after the addition of CB. A similar pattern was observed on the lactate level: after addition of CB the production of lactate decreased by 25%. The results of this study showed real-time cell metabolism detection, enabling the use of this platform in drug screening applications (Table 5).

Some cancers have the ability to grow and metastasize to different parts of the body. This process is possible because of the release of tumor cells from the primary tumor location through the bloodstream or lymphatic system [112,113]. These circulating tumor cells can provide information about the original tumor and, therefore, can be relevant for cancer diagnostics [114]. Metastasis of breast cancer cells was investigated in a microfluidic chip with integrated electrical cell impedance-sensing technology [115]. The device comprised microelectrode arrays, cell capture arrays, and a microfluidic channel, where cells were trapped on top of working electrodes (Fig. 5c). Breast cancer cells MDA-MB-231 and MCF-7 were placed inside the microfluidic-integrated biosensor in the presence of Matrigel™. Measurements of impedance were

TABLE 4
Biomarkers as targets for diagnostic purposes^a

Cancer	Biomarkers
Bladder	miR-126, miR-141-3p, NMP22, FDP, IL-8, hOGG1, COX-2, BTA
Brain	miR-10b, MGMT, COX-2, p14arf
Breast	miR-155, miR-261, CA15-3, EGFR, VEGF165, BRCA I, ErbB2, HER2, mucin-1, ER, PR, HER 2, uPA and PAI-1, BRCA-1, BRCA-2, cathepsin D, ING-1, CA 27-29
Liver	AFP, DCP, TGF-beta-1, GGT, CEA
Lung	miR-106a-5p, miR-10b-5p, miR-141-3p, KRAS, ALP, CEA, EGFR, NSE, CEA, RBP
Prostate	EPCA, IGFBP-2TGF-β1, IL-6
Testicular	AFP, hCG

^aAbbreviations: miR, MicroRNA; NMP, Nuclear Matrix Protein; FDP, Fibrin Degradation Protein; IL, Interleukin; hOGG1, 8-oxoguanine DNA glycosylase; COX, Cyclooxygenase; BTA, Bladder Tumor Antigen; MGMT, O-6-methylguanine-DNA methyltransferase; ARF, Alternate Reading Frame Protein; CA, Cancer Antigen; EGFR, Epidermal Growth Factor Receptor; VEGF, Vascular Endothelial Growth Factor; BRCA, Breast Cancer Gene; Erb, Erythroblast Leukemia Viral Oncogene; HER, Human Epidermal Growth Factor; ER, Estrogen Receptor; PR, Progesterone Receptor; uPA, Urokinase Plasminogen Activator; PAI, Plasminogen Activator Inhibitor; ING, Inhibitor of Growth Protein, AFP, Alpha-fetoprotein; DCP, Des-gamma-carboxy prothrombin; TGF, Transforming Growth Factor; GGT, Gamma-glutamyl transferase; CEA, Carcinoembryonic Antigen; KRAS, Kirsten rat sarcoma oncogene; ALP, Alkaline Phosphatase; NSE, Neuron-specific Enolase; RBP, Retinol-binding Protein; EPCA, Early Prostate Cancer Antigen; IGFBP, Insulin-like Growth Factor-binding Protein; TGF, Transforming Growth Factor; hCG, Human Chorionic Gonadotropin.



Drug Discovery Today

FIGURE 5

Biosensors for cancer research. **(a)** On-chip oxygen and chemical concentration gradient device for studying tumor–drug interactions in a tumor microenvironment (left). The change in color shows the creation of a chemical concentration gradient by two dyes between two terminals (right). **(b)** Multisensor microfluidic device composed of cell culture chamber and chemical and biological sensors (top left). Microscopic image of T98G human brain cancer cells growing inside the cell culture chamber (top right). Change in pH (bottom left) and lactate level (bottom right) on cellular metabolism of T98G cells after addition of cytochalasin B. **(c)** Microfluidic chip with integrated electrical cell impedance sensing to monitor migration of breast cancer cells. The chip comprised microelectrode arrays (MEAs), cell capture arrays (CCAs), and a microfluidic channel. Change in impedance was seen as a result of cell migration. **(d)** Microfluidic plasmonic biosensor for detection of breast cancer HER2 antigen (left) by immobilization of HER2 antibody AB1 on gold film (right). **(e)** High-throughput electrochemical microfluidic immunoarray with 32-sensor configuration (left) and 256-sensor system (right). **(f)** Automated microfluidic platform of bead-based electrochemical immunosensor integrated with liver bioreactor for continual monitoring of target biomarkers. Reprinted, with permission, from [102] (a), [111] (b), [115] (c), [117] (d), [118] (e), and [119] (f).

TABLE 5

Microfluidic-integrated biosensors for cancer drug studies

Cancer	Contribution of sensing technology	Refs
Lung cancer (A549) and cervical carcinoma (HeLa)	PDMS mixed with platinum octaethylporphyrin dye created a permeable membrane able to measure oxygen consumption during administration of anticancer drugs	[102]
Brain cancer (T98G)	Integration of chemical (pH and oxygen) and biological (lactate and glucose) sensors allowed real-time detection of cell metabolism changes when medium was altered	[111]
Breast cancer (MDA-MD-231)	Integration of electrical cell-impedance sensor allowed measurement of impedance and correlation with migration behavior of cancer cells	[115]
HER2 antigen	AB1-surface immobilized gold nanohole array was created inside a microfluidic device, allowing real-time HER2 antigen detection with high sensitivity	[117]
Prostate cancer biomarkers	Magnetic nanoparticles were decorated with secondary antibodies achieved high sensitivity in detection of prostate biomarker proteins in serum	[118]
Prostate biomarkers	Automated microfluidic bead-based electrochemical immunosensor with magnetic microbeads immobilized with biomarker-recognition molecules enabled continual on-chip detection of secreted biomarkers from hepatocytes	[119]

correlated with the migration behavior of the breast cancer cells. MDA-MB-231 showed a rapid variation of impedance magnitude, whereas no change was seen for the less-metastatic MCF-7 cells. The proposed microfluidic device allowed for fast and real-time selective detection of migratory properties of cancer cells.

Biosensing technology has also been used in the detection of cancer biomarkers, owing to the potential of early cancer detection [116]. A microfluidic plasmonic biosensor developed by Monteiro *et al.* was able to detect low levels of HER2 antigen [117]. HER2 antibody AB1 was immobilized on the surface of a gold nanohole array, creating a biorecognizing element in the chip (Fig. 5d). Immobilization of HER2 was verified with the aid of a spectrometer, where transmitted light was collected by an optical fiber. To verify the functionality of the device, HER2 antigen was flowed onto the chip, followed by the addition of AB2 antibody, to improve the sensitivity of the optical sensor. A concentration of 30 ng/ml was detected in the platform, showing the potential of this device for cancer diagnosis.

Current standard techniques for quantification of proteins, for example ELISA, are reagent costly and the signal amplification is minimal. To provide a high degree of multiplexing for protein detection, a high-throughput microfluidic electrochemical immunosensor system was developed (Fig. 5e) [118]. The device comprised a 32-sensor array that could be integrated into a modular microfluidic device, combining up to 256 immunosensors for a cost of less than US\$200. The detection of proteins was possible by using magnetic nanoparticles labeled with secondary antibodies inside the fluidic chamber. Analysis of prostate cancer biomarker proteins, such as prostate-specific antigen (PSA), IL-6, and platelet factor-4 (PF-4), performed using the 256-sensor system showed good correlation with single-protein ELISA results, demonstrating the biosensing potential of the microfluidic device.

In a similar approach, Riahi *et al.* developed a microfluidic platform of bead-based electrochemical immunosensors (Fig. 5f) [119]. This platform was connected to a microfluidic liver bioreactor, where human primary hepatocyte spheroids were administered with acetaminophen to monitor protein secretion. In addition to the capability to continually monitor the secreted biomarkers, the electrochemical immunosensor showed a limit of detection of one order of magnitude better than ELISA (0.03 ng/ml on the microfluidic device compared with 0.2 ng/ml on ELISA) [119].

There has been extensive progress over the years regarding the development of label-free and label-based high-throughput biosensors for multiparametric sensing of tumor functions. These sensors have not only sensed biomarkers and quantified biophysical conditions of the tumor microenvironment, but also found their applications in drug discovery and screening. Future biosensors can bring further sophistication by miniaturizing the device and integrating the sensing elements for the detection of biophysical and biochemical features of the tumor microenvironment in a fully integrated HTS platform. In addition, the integration of biosensors to microfluidic technology can potentially provide point-of-care devices as a solution for management of cancer diagnosis [120,121].

Concluding remarks and future perspectives

Microfluidic devices have been shown to be excellent platforms to create 3D cell culture models for drug discovery. The small dimensions of the channels allow for spatial and temporal control of the system under study while closely mimicking the environment inside the human body in an *in vitro* device. In addition, microfluidic devices are cost-effective because only microliter volumes of reagents are required. Microfabrication techniques used in the development process of microfluidic devices allow for flexibility in terms of the design of the platform. Therefore, numerous additions can be made to the regular design of a tumor-on-a-chip, because of the inclusion of a CGG that allows combinatory cytotoxicity studies and the addition of biosensors that permit qualitative and quantitative on-chip analysis, transforming the platform into a time-efficient, high-throughput microfluidic assay. In addition, microfluidic technology allows the integration of individual microfluidic devices to recreate a body-on-a-chip for the study of more-complex physiological responses of tissues and organs [122]. The interconnection between cancerous tissues and organs allows a more realistic investigation of drug efficacy during the development of new therapeutic drugs, narrowing the response gap between *in vivo* and *in vitro* models [123].

Even though considerable progress in the development of 3D *in vitro* cell cultures has been made using microfluidics, some challenges are still to overcome. Although the small channels allow the use of small sample volumes, the number of cells inside the chip is not high. Therefore, highly sensitive analysis methods are required to evaluate samples collected from cell cultures.

Microfabrication based on the production of a patterned master for PDMS molding is a feasible technique to be used in a laboratory. However, large-scale manufacturing of microfluidic devices is still a challenge and will require new fabrication strategies using more low-cost materials. PDMS-based microfluidic devices also show some fragility when handling, where small pressure variation on the PDMS can create an irreversible impact on the cell culture inside the device. In addition, PDMS is known to adsorb small hydrophilic molecules and, consequently, it can alter the results obtained in the platform [89]. Therefore, alternative materials and new fabrication strategies are still required for the large-scale production of microfluidic devices for biological applications. 3D printers can be an excellent alternative to the photolithography processes [124,125]. However, it is still a challenge to obtain completely optical transparency and biocompatibility in 3D-printed microfluidic devices.

There is still a gap between the use of microfluidic devices in cell studies and the commercial use of these platforms due to a lack of standardization [61,63]. Although numerous microfluidic devices are available, most chips are designed to study a specific cell interaction or metabolism. Therefore, the translation of these platforms to a commercial, standardized device is still far from reality. In addition, some microfluidic devices still require the attachment of specialized equipment, such as syringe pumps, lasers, and mass spectrometers, which are not easily available in most laboratories [126]. Therefore, the development of on-chip analysers and detection systems would allow the creation of more user-friendly platforms. However, bearing in mind that a standardized platform might be difficult to achieve since some studies might not require a high level architectural complexity on the

chip, the fabrication of a modular ‘plug and play’ platform could be the best approach toward standardization [127].

In addition, owing to a lack of validation, there is still a bridge between studies performed on microfluidic platforms and the use of these platforms in the drug discovery process [13,62]. The response obtained in these platforms needs to be validated with *in vivo* responses. However, comparison with animal models is not enough because animal cells behave and respond differently to human cells. The responses obtained in microfluidic platforms need to be compared to clinical trial outcomes for better validation. In addition, primary human cells instead of cancerous cell lines should be used in the studies performed using microfluidic devices to mimic *in vivo* responses closely.

The development of multiculture systems remains a challenge to microfluidics. The use of multiple cell lines requires the perfusion of different growth media because each cell culture requires specific growth factors and nutrients. Microfluidic devices with individually compartmentalized channels have been used in the creation of 3D multiculture models, where each cell line is cultured in separated channels with individual perfusion inlets. However, there is still a need to find a universal growth medium that can be used to perfuse the entire device, especially to be applied to the modular microfluidic platforms.

Acknowledgments

M.A. and A.S.N. would like to thank the Natural Sciences and Engineering Research Council of Canada and Canadian Foundation for Innovation for supporting this work. A.S. would like to thank the National Sciences and Engineering Research Council Chair Program for supporting this work.

References

- 1 American Cancer Society (2016) *Cancer Facts & Figures 2016*. American Cancer Society
- 2 National Cancer Institute (2016) *Cancer Statistics*. National Cancer Institute
- 3 McKinnell, R.G. *et al.* eds (2006) *The Biological Basis of Cancer*, Cambridge University Press
- 4 Pardee, A.B. and Stein, G.S., eds (2008) *The Biology and Treatment of Cancer: Understanding Cancer*, John Wiley & Sons
- 5 Guan, X. (2015) Cancer metastases: challenges and opportunities. *Acta Pharm. Sin. B* 5, 402–418
- 6 Steeg, P.S. (2016) Targeting metastasis. *Nat. Rev. Cancer* 16, 201–218
- 7 Khan, I.U. *et al.* (2013) Microfluidics: a focus on improved cancer targeted drug delivery systems. *J. Control. Release* 172, 1065–1074
- 8 Nyga, A. *et al.* (2011) 3D tumour models: novel *in vitro* approaches to cancer studies. *J. Cell Commun. Signal.* 5, 239–248
- 9 Wu, M.-H. *et al.* (2010) Microfluidic cell culture systems for drug research. *Lab Chip* 10, 939
- 10 Zheng, X.T. *et al.* (2013) On-chip investigation of cell–drug interactions. *Adv. Drug Deliv. Rev.* 65, 1556–1574
- 11 Sackmann, E.K. *et al.* (2014) The present and future role of microfluidics in biomedical research. *Nature* 507, 181–189
- 12 Kim, J.B. *et al.* (2004) Three-dimensional *in vitro* tissue culture models of breast cancer—a review. *Breast Cancer Res. Treat.* 85, 281–291
- 13 Zhang, Z. and Nagrath, S. (2013) Microfluidics and cancer: are we there yet? *Biomed. Microdevices* 15, 595–609
- 14 Polini, A. *et al.* (2014) Organs-on-a-chip: a new tool for drug discovery. *Expert Opin. Drug Discov.* 9, 335–352
- 15 Ghaemmaghami, A.M. *et al.* (2012) Biomimetic tissues on a chip for drug discovery. *Drug Discov. Today* 17, 173–181
- 16 Bhatia, S.N. and Ingber, D.E. (2014) Microfluidic organs-on-chips. *Nat. Biotechnol.* 32, 760–772
- 17 Whitesides, G.M. (2006) The origins and the future of microfluidics. *Nature* 442, 368–373
- 18 Quail, D.F. and Joyce, J.A. (2013) Microenvironmental regulation of tumor progression and metastasis. *Nat. Med.* 19, 1423–1437
- 19 Wilson, W.R. and Hay, M.P. (2011) Targeting hypoxia in cancer therapy. *Nat. Rev. Cancer* 11, 393–410
- 20 Lu, P. *et al.* (2012) The extracellular matrix: a dynamic niche in cancer progression. *J. Cell Biol.* 196, 395–406
- 21 Butcher, D.T. *et al.* (2009) A tense situation: forcing tumour progression. *Nat. Rev. Cancer* 9, 108–122
- 22 Frantz, C. *et al.* (2010) The extracellular matrix at a glance. *J. Cell Sci.* 123, 4195–4200
- 23 Berean, K. *et al.* (2014) The effect of crosslinking temperature on the permeability of PDMS membranes: evidence of extraordinary CO₂ and CH₄ gas permeation. *Sep. Purif. Technol.* 122, 96–104
- 24 Minchinton, A.I. and Tannock, I.F. (2006) Drug penetration in solid tumours. *Nat. Rev. Cancer* 6, 583–592
- 25 Hanahan, D. and Weinberg, R.A. (2011) Hallmarks of cancer: the next generation. *Cell* 144, 646–674
- 26 Munson, J.M. and Shieh, A.C. (2014) Interstitial fluid flow in cancer: implications for disease progression and treatment. *Cancer Manag. Res.* 6, 317–328
- 27 Polacheck, W.J. *et al.* (2013) Tumor cell migration in complex microenvironments. *Cell. Mol. Life Sci.* 70, 1335–1356
- 28 Trédan, O. *et al.* (2007) Drug resistance and the solid tumor microenvironment. *J. Natl. Cancer Inst.* 99, 1441–1454
- 29 Heldin, C.-H. *et al.* (2004) High interstitial fluid pressure – an obstacle in cancer therapy. *Nat. Rev. Cancer* 4, 806–813
- 30 Salnikov, A.V. *et al.* (2003) Lowering of tumor interstitial fluid pressure specifically augments efficacy of chemotherapy. *FASEB J.* 17, 1756–1758

- 31 Chiche, J. *et al.* (2010) Tumour hypoxia induces a metabolic shift causing acidosis: a common feature in cancer. *J. Cell. Mol. Med.* 14, 771–794
- 32 Eales, K.L. *et al.* (2016) Hypoxia and metabolic adaptation of cancer cells. *Oncogenesis* 5, e190
- 33 Nishida, N. *et al.* (2006) Angiogenesis in cancer. *Vasc. Health Risk Manag.* 2, 213–219
- 34 Weis, S.M. and Cheresh, D.A. (2011) Tumor angiogenesis: molecular pathways and therapeutic targets. *Nat. Med.* 17, 1359–1370
- 35 Infanger, D.W. *et al.* (2013) Engineered culture models for studies of tumor-microenvironment interactions. *Annu. Rev. Biomed. Eng.* 15, 29–53
- 36 Folkman, J. (2002) Role of angiogenesis in tumor growth and metastasis. *Semin. Oncol.* 29, 15–18
- 37 Pampaloni, F. *et al.* (2007) The third dimension bridges the gap between cell culture and live tissue. *Nat. Rev. Mol. Cell Biol.* 8, 839–845
- 38 Xu, X. *et al.* (2014) Three-dimensional *in vitro* tumor models for cancer research and drug evaluation. *Biotechnol. Adv.* 32, 1256–1268
- 39 Breslin, S. and O'Driscoll, L. (2013) Three-dimensional cell culture: the missing link in drug discovery. *Drug Discov. Today* 18, 240–249
- 40 Kim, J.B. (2005) Three-dimensional tissue culture models in cancer biology. *Semin. Cancer Biol.* 15, 365–377
- 41 Ivascu, A. and Kubbies, M. (2006) Rapid generation of single-tumor spheroids for high-throughput cell function and toxicity analysis. *J. Biomol. Screen.* 11, 922–932
- 42 Tung, Y.-C. *et al.* (2011) High-throughput 3D spheroid culture and drug testing using a 384 hanging drop array. *Analyst* 136, 473–478
- 43 Gupta, N. *et al.* (2016) Microfluidics-based 3D cell culture models: utility in novel drug discovery and delivery research. *Bioeng. Transl. Med.* 1, 63–81
- 44 Pickl, M. and Ries, C.H. (2009) Comparison of 3D and 2D tumor models reveals enhanced HER2 activation in 3D associated with an increased response to trastuzumab. *Oncogene* 28, 461–468
- 45 Katt, M.E. *et al.* (2016) *In vitro* tumor models: advantages, disadvantages, variables, and selecting the right platform. *Front. Bioeng. Biotechnol.* 4, 1–14
- 46 Mehta, G. *et al.* (2012) Opportunities and challenges for use of tumor spheroids as models to test drug delivery and efficacy. *J. Control. Release* 164, 192–204
- 47 Huttmacher, D.W. (2010) Biomaterials offer cancer research the third dimension. *Nat. Mater.* 9, 90–93
- 48 Chan, B.P. and Leong, K.W. (2008) Scaffolding in tissue engineering: general approaches and tissue-specific considerations. *Eur. Spine J.* 17 (Suppl. 4), 467–479
- 49 Chen, F.-M. and Liu, X. (2016) Advancing biomaterials of human origin for tissue engineering. *Prog. Polym. Sci.* 53, 86–168
- 50 Okamoto, M. and John, B. (2013) Synthetic biopolymer nanocomposites for tissue engineering scaffolds. *Prog. Polym. Sci.* 38, 1487–1503
- 51 Tamayol, A. *et al.* (2013) Fiber-based tissue engineering: progress, challenges, and opportunities. *Biotechnol. Adv.* 31, 669–687
- 52 Nam, Y.S. and Park, T.G. (1999) Biodegradable polymeric microcellular foams by modified thermally induced phase separation method. *Biomaterials* 20, 1783–1790
- 53 Ghorbanian, S. *et al.* (2014) Microfluidic direct writer with integrated declogging mechanism for fabricating cell-laden hydrogel constructs. *Biomed. Microdevices* 16, 387–395
- 54 Akbari, M. *et al.* (2016) Textile technologies and tissue engineering: a path toward organ weaving. *Adv. Healthc. Mater.* 5, 751–766
- 55 Annabi, N. *et al.* (2014) 25th Anniversary Article: Rational design and applications of hydrogels in regenerative medicine. *Adv. Mater.* 26, 85–124
- 56 Kharaziha, M. *et al.* (2016) Nano-enabled approaches for stem cell-based cardiac tissue engineering. *Adv. Healthc. Mater.* 5, 1533–1553
- 57 Chen, L. *et al.* (2012) The enhancement of cancer stem cell properties of MCF-7 cells in 3D collagen scaffolds for modeling of cancer and anti-cancer drugs. *Biomaterials* 33, 1437–1444
- 58 Casey, A. *et al.* (2016) Chemotherapeutic efficiency of drugs *in vitro*: comparison of doxorubicin exposure in 3D and 2D culture matrices. *Toxicol. In Vitro* 33, 99–104
- 59 Cavo, M. *et al.* (2016) Microenvironment complexity and matrix stiffness regulate breast cancer cell activity in a 3D *in vitro* model. *Sci. Rep.* 6, 1–13
- 60 O'Brien, F.J. (2011) Biomaterials & scaffolds for tissue engineering. *Mater. Today* 14, 88–95
- 61 van der Meer, A.D. and van den Berg, A. (2012) Organs-on-chips: breaking the *in vitro* impasse. *Integr. Biol. (Camb)* 4, 461–470
- 62 Huh, D. *et al.* (2011) From 3D cell culture to organs-on-chips. *Trends Cell Biol.* 21, 745–754
- 63 Selimović, S. *et al.* (2013) Organs-on-a-chip for drug discovery. *Curr. Opin. Pharmacol.* 13, 829–833
- 64 Tian, W.C. and Finehout, E., eds (2009) *Microfluidics for Biological Applications*, Springer, US
- 65 Karimi, M. *et al.* (2016) Microfluidic systems for stem cell-based neural tissue engineering. *Lab Chip* 16, 2551–2571
- 66 Mohammadi, M.H. *et al.* (2016) Skin diseases modeling using combined tissue engineering and microfluidic technologies. *Adv. Healthc. Mater.* 5, 2459–2480
- 67 Hasan, A. *et al.* (2014) Microfluidic techniques for development of 3D vascularized tissue. *Biomaterials* 35, 7308–7325
- 68 Huang, C.P. *et al.* (2009) Engineering microscale cellular niches for three-dimensional multicellular co-cultures. *Lab Chip* 9, 1740–1748
- 69 Choi, Y. *et al.* (2015) A microengineered pathophysiological model of early-stage breast cancer. *Lab Chip* 15, 3350–3357
- 70 Bersini, S. *et al.* (2014) A microfluidic 3D *in vitro* model for specificity of breast cancer metastasis to bone. *Biomaterials* 35, 2454–2461
- 71 Chung, S. *et al.* (2010) Microfluidic platforms for studies of angiogenesis, cell migration, and cell-cell interactions. *Ann. Biomed. Eng.* 38, 1164–1177
- 72 Shin, Y. *et al.* (2012) Microfluidic assay for simultaneous culture of multiple cell types on surfaces or within hydrogels. *Nat. Protoc.* 7, 1247–1259
- 73 Jeon, J.S. *et al.* (2013) *In vitro* model of tumor cell extravasation. *PLoS One* 8, e56910
- 74 Hsu, Y.-L. *et al.* (2013) Breast tumor-associated osteoblast-derived CXCL5 increases cancer progression by ERK/MSK1/Elk-1/snail signaling pathway. *Oncogene* 32, 4436–4447
- 75 Xu, Z. *et al.* (2016) Design and construction of a multi-organ microfluidic chip mimicking the *in vivo* microenvironment of lung cancer metastasis. *ACS Appl. Mater. Interfaces* 8, 25840–25847
- 76 Ma, H. *et al.* (2013) Biomimetic tumor microenvironment on a microfluidic platform. *Biomicrofluidics* 7, 11501–11513
- 77 Young, E.W.K. (2013) Cells, tissues, and organs on chips: challenges and opportunities for the cancer tumor microenvironment. *Integr. Biol. (Camb)* 5, 1096–1109
- 78 Ye, N. *et al.* (2007) Cell-based high content screening using an integrated microfluidic device. *Lab Chip* 7, 1696–1704
- 79 Xu, Z. *et al.* (2013) Application of a microfluidic chip-based 3D co-culture to test drug sensitivity for individualized treatment of lung cancer. *Biomaterials* 34, 4109–4117
- 80 Li, M.C. *et al.* (1960) Effects of combined drug therapy on metastatic cancer of the testis. *JAMA* 174, 1291–1299
- 81 Bonadonna, G. *et al.* (1976) Combination chemotherapy as an adjuvant treatment in operable breast cancer. *N. Engl. J. Med.* 294, 405–410
- 82 Burris, H.A. *et al.* (1997) Improvements in survival and clinical benefit with gemcitabine as first-line therapy for patients with advanced pancreas cancer: a randomized trial. *J. Clin. Oncol.* 15, 2403–2413
- 83 Ding, Y. *et al.* (2015) Microfluidic-enabled print-to-screen platform for high-throughput screening of combinatorial chemotherapy. *Anal. Chem.* 87, 10166–10171
- 84 Sabhachandani, P. *et al.* (2016) Generation and functional assessment of 3D multicellular spheroids in droplet based microfluidics platform. *Lab Chip* 16, 497–505
- 85 Esch, E.W. *et al.* (2015) Organs-on-chips at the frontiers of drug discovery. *Nat. Rev. Drug Discov.* 14, 248–260
- 86 Inamdar, N.K. and Borenstein, J.T. (2011) Microfluidic cell culture models for tissue engineering. *Curr. Opin. Biotechnol.* 22, 681–689
- 87 Halldórsson, S. *et al.* (2015) Advantages and challenges of microfluidic cell culture in polydimethylsiloxane devices. *Biosens. Bioelectron.* 63, 218–231
- 88 Wang, J.D. *et al.* (2012) Quantitative analysis of molecular absorption into PDMS microfluidic channels. *Ann. Biomed. Eng.* 40, 1862–1873
- 89 Toepke, M.W. and Beebe, D.J. (2006) PDMS absorption of small molecules and consequences in microfluidic applications. *Lab Chip* 6, 1484–1486
- 90 Fan, Y. *et al.* (2016) Engineering a brain cancer chip for high-throughput drug screening. *Sci. Rep.* 6, 1–12
- 91 Luka, G. *et al.* (2015) Microfluidics integrated biosensors: a leading technology towards lab-on-a-chip and sensing applications. *Sensors* 15, 30011–30031
- 92 Bell, A.A. *et al.* (2009) High dynamic range microscopy for cytopathological cancer diagnosis. *IEEE J. Sel. Top. Signal Process.* 3, 170–184
- 93 Jung, W. *et al.* (2015) Point-of-care testing (POCT) diagnostic systems using microfluidic lab-on-a-chip technologies. *Microelectron. Eng.* 132, 46–57
- 94 Costa-Pinheiro, P. *et al.* (2015) Diagnostic and prognostic epigenetic biomarkers in cancer. *Epigenomics* 7, 1003–1015
- 95 Schwarzenbach, H. *et al.* (2014) Clinical relevance of circulating cell-free microRNAs in cancer. *Nat. Rev. Clin. Oncol.* 11, 145–156
- 96 Zhang, Y. *et al.* (2013) Early lung cancer diagnosis by biosensors. *Int. J. Mol. Sci.* 14, 15479–15509
- 97 Srinivas, P.R. *et al.* (2001) Trends in biomarker research for cancer detection. *Lancet Oncol.* 2, 698–704
- 98 Zare, R.N. and Kim, S. (2010) Microfluidic platforms for single-cell analysis. *Annu. Rev. Biomed. Eng.* 12, 187–201
- 99 El-Ali, J. *et al.* (2006) Cells on chips. *Nature* 442, 403–411

- 100 Stroock, A.D. and Whitesides, G.M. (2002) Components for integrated poly (dimethylsiloxane) microfluidic systems. *Electrophoresis* 23, 3461–3473
- 101 Reshkin, S.J. *et al.* (2013) Na⁺-H⁺ exchanger, pH regulation and cancer. *Recent Pat. Anticancer Drug Discov.* 8, 85–99
- 102 Wang, L. *et al.* (2013) Construction of oxygen and chemical concentration gradients in a single microfluidic device for studying tumor cell–drug interactions in a dynamic hypoxia microenvironment. *Lab Chip* 13, 695–705
- 103 Lambrechts, D. *et al.* (2013) Fluorescent oxygen sensitive microbead incorporation for measuring oxygen tension in cell aggregates. *Biomaterials* 34, 922–929
- 104 Dmitriev, R.I. *et al.* (2015) Versatile conjugated polymer nanoparticles for high-resolution O₂ imaging in cells and 3D tissue models. *ACS Nano* 9, 5275–5288
- 105 Kasinskas, R.W. *et al.* (2014) Rapid uptake of glucose and lactate, and not hypoxia, induces apoptosis in three-dimensional tumor tissue culture. *Integr. Biol.* 6, 399–410
- 106 Torino, F. *et al.* (2013) Circulating tumor cells in colorectal cancer patients. *Cancer Treat. Rev.* 39, 759–772
- 107 Ding, C. and Tian, Y. (2015) Gold nanocluster-based fluorescence biosensor for targeted imaging in cancer cells and ratiometric determination of intracellular pH. *Biosens. Bioelectron.* 65, 183–190
- 108 Pui, T.S. *et al.* (2013) Detection of tumor necrosis factor (TNF- α) in cell culture medium with label free electrochemical impedance spectroscopy. *Sens. Actuators B Chem.* 181, 494–500
- 109 Ma, X. *et al.* (2014) Ultra-pH-sensitive nanoprobe library with broad pH tunability and fluorescence emissions. *J. Am. Chem. Soc.* 136, 11085–11092
- 110 Madsen, J. *et al.* (2013) Nile blue-based nanosized pH sensors for simultaneous far-red and near-infrared live bioimaging. *J. Am. Chem. Soc.* 135, 14863–14870
- 111 Weltin, A. *et al.* (2014) Cell culture monitoring for drug screening and cancer research: a transparent, microfluidic, multi-sensor microsystem. *Lab Chip* 14, 138–146
- 112 Pantel, K. and Speicher, M.R. (2016) The biology of circulating tumor cells. *Oncogene* 35, 1216–1224
- 113 Alix-Panabières, C. and Pantel, K. (2014) Challenges in circulating tumour cell research. *Nat. Rev. Cancer* 14, 623–631
- 114 Williams, S.C.P. (2013) Circulating tumor cells. *Proc. Natl. Acad. Sci. U. S. A.* 110, 4861
- 115 Nguyen, T.A. *et al.* (2013) Microfluidic chip with integrated electrical cell-impedance sensing for monitoring single cancer cell migration in three-dimensional matrixes. *Anal. Chem.* 85, 11068–11076
- 116 Munge, B.S. *et al.* (2016) Multiplex immunosensor arrays for electrochemical detection of cancer biomarker proteins. *Electroanalysis* 28, 2644–2658
- 117 Monteiro, J.P. *et al.* (2016) Microfluidic plasmonic biosensor for breast cancer antigen detection. *Plasmonics* 11, 45–51
- 118 Tang, C.K. *et al.* (2016) High-throughput electrochemical microfluidic immunoarray for multiplexed detection of cancer biomarker proteins. *ACS Sensors* 1, 1036–1043
- 119 Riahi, R. *et al.* (2016) Automated microfluidic platform of bead-based electrochemical immunosensor integrated with bioreactor for continual monitoring of cell secreted biomarkers. *Sci. Rep.* 6, 1–14
- 120 Mross, S. *et al.* (2015) Microfluidic enzymatic biosensing systems: a review. *Biosens. Bioelectron.* 70, 376–391
- 121 Escobedo, C. (2013) On-chip nanohole array based sensing: a review. *Lab Chip* 13, 2445–2463
- 122 Skardal, A. *et al.* (2016) Organoid-on-a-chip and body-on-a-chip systems for drug screening and disease modeling. *Drug Discov. Today* 21, 1399–1411
- 123 Perestrelo, A. *et al.* (2015) Microfluidic organ/body-on-a-chip devices at the convergence of biology and microengineering. *Sensors* 15, 31142–31170
- 124 Ho, C.M.B. *et al.* (2015) 3D printed microfluidics for biological applications. *Lab Chip* 15, 3627–3637
- 125 Waheed, S. *et al.* (2016) 3D printed microfluidic devices: enablers and barriers. *Lab Chip* 16, 1993–2013
- 126 Ying, L. and Wang, Q. (2013) Microfluidic chip-based technologies: emerging platforms for cancer diagnosis. *BMC Biotechnol.* 13, 1–10
- 127 Meng, Z.-J. *et al.* (2015) Plug-n-play microfluidic systems from flexible assembly of glass-based flow-control modules. *Lab Chip* 15, 1869–1878
- 128 Swartz, M.A. and Lund, A.W. (2012) Lymphatic and interstitial flow in the tumour microenvironment: linking mechanobiology with immunity. *Nat. Rev. Cancer* 12, 210–219
- 129 Zetter, B.R. (2008) The scientific contributions of M. Judah Folkman to cancer research. *Nat. Rev. Cancer* 8, 647–654
- 130 Schroeder, A. *et al.* (2012) Treating metastatic cancer with nanotechnology. *Nat. Rev. Cancer* 12, 39–50